# Calculation of OTF, NPS, and DQE for Oblique X-Ray Incidence on Turbid Granular Phosphors

Raymond J. Acciavatti and Andrew D.A. Maidment

University of Pennsylvania, Department of Radiology, Physics Section, 1 Silverstein Building, 3400 Spruce St., Philadelphia PA 19104-4206
racci@seas.upenn.edu, Andrew.Maidment@uphs.upenn.edu

**Abstract.** Digital breast tomosynthesis (DBT) is an imaging modality in which tomographic sections of the breast are generated from a limited range of x-ray tube angles. One drawback of DBT is resolution loss in the oblique projection images. The purpose of this work is to extend Swank's formulation of the transfer functions of turbid granular phosphors to oblique x-ray incidence, using the diffusion approximation to the Boltzmann equation to model the spread of light in the phosphor. As expected, the modulation transfer function (MTF) and noise power spectra (NPS) are found to decrease with projection angle regardless of frequency. By contrast, the dependence of detective quantum efficiency (DQE) on projection angle is frequency dependent. DQE increases with projection angle at low frequencies, and only decreases with projection angle at high frequencies. Importantly, the x-ray quantum detection efficiency ($A_Q$) and the Swank information factor ($A_S$) are also found to be angularly dependent.

**Keywords:** Digital breast tomosynthesis (DBT), oblique x-ray incidence, turbid granular phosphor, optical transfer function (OTF), modulation transfer function (MTF), noise power spectra (NPS), detective quantum efficiency (DQE), Swank information factor ($A_S$).

## 1 Introduction

Digital breast tomosynthesis (DBT) is an emerging 3D imaging modality in which x-ray images of the compressed breast are acquired over a limited range of projection angles. Using digital image reconstruction techniques, tomographic sections at all depths of the breast volume can then be generated. Preliminary studies indicate that DBT provides increased sensitivity and specificity for the early detection of breast cancer in women relative to conventional 2D digital mammography [1].

One trade-off of DBT is resolution loss in the projection images as a result of oblique x-ray incidence. Although the degradation in image quality due to oblique x-ray incidence has been studied in columnar cesium iodide phosphors doped with thallium (CsI:Tl) with empirical data [2] and amorphous selenium (*a*-Se) direct converting detectors using Monte Carlo simulations [3], to our knowledge no one has performed a theoretical analysis of the consequences of oblique x-ray incidence. The purpose of this work is to extend Swank's analytical formulation [4] of the transfer functions of x-ray fluorescent screens to oblique x-ray incidence. To this end, we have considered a non-structured turbid granular phosphor such as gadolinium oxysulfide

J. Martí et al. (Eds.): IWDM 2010, LNCS 6136, pp. 436–443, 2010.

doped with terbium ($Gd_2O_2S$:Tb), which is commonly used in breast imaging and which can reasonably approximate other detector materials.

## 2 Methods

The optical transfer function (OTF), noise power spectra (NPS), and detective quantum efficiency (DQE) of a turbid granular phosphor irradiated obliquely are now derived from first principles. The spread of visible light in a scintillator can be described by the Boltzmann transport equation. A first-order, steady state solution to the Boltzmann transport equation is a diffusion equation of the form [5]

$$-\nabla^2\phi(\mathbf{r})+\sigma^2\phi(\mathbf{r})=S(\mathbf{r}) \ , \tag{1}$$

where $\phi(\mathbf{r})$ is the product of the density of the secondary carriers (*i.e.*, the optical photons) with the diffusion constant, σ is the reciprocal of the mean diffusion length of the secondary carriers, and $S(\mathbf{r})$ is the source function. The source function $S(\mathbf{r})$ may be modeled as point-like and positioned on $(z_0\tan\theta, 0, z_0)$, where $z_0$ is the depth of the phosphor of total thickness $T$ and where $\theta$ is the projection angle relative to normal x-ray incidence. In terms of Dirac delta functions, $S(\mathbf{r})$ can be written as

$$S(\mathbf{r})=\delta(x-z_0\tan\theta)\delta(y)\delta(z-z_0) \ . \tag{2}$$

In the Fourier domain, the source function can be written as the integral

$$S(\mathbf{r})=\delta(z-z_0)\int_{-\infty}^{\infty}\int_{-\infty}^{\infty}e^{2\pi i[(x-z_0\tan\theta)\nu_x+y\nu_y]}d\nu_x d\nu_y \ . \tag{3}$$

Assuming solutions to Eq. (1) of the form

$$\phi(x,y,z)=\int_{-\infty}^{\infty}\int_{-\infty}^{\infty}\psi_{\mathbf{k}}(z)e^{2\pi i(x\nu_x+y\nu_y)}d\nu_x d\nu_y \ , \tag{4}$$

one finds

$$-\frac{d^2\psi_{\mathbf{k}}}{dz^2}+q^2\psi_{\mathbf{k}}=e^{-ik_x z_0\tan\theta}\delta(z-z_0) \ , \quad q^2=\sigma^2+k_x^2+k_y^2 \ , \tag{5}$$

where $\boldsymbol{\nu}$ is the 2D spatial frequency vector and $\mathbf{k} = 2\pi\boldsymbol{\nu}$. To solve this differential equation, one can apply integral transform techniques. Denoting the Laplace transform of $\psi_{\mathbf{k}}(z)$ as $\Psi_{\mathbf{k}}(p)$, the transform of the differential equation is

$$(-p^2+q^2)\Psi_{\mathbf{k}}(p)+C_1p+C_2=e^{-ik_x z_0\tan\theta}e^{-pz_0} \ , \tag{6}$$

where $C_1$ and $C_2$ are the constants of integration. Solving for $\Psi_{\mathbf{k}}(p)$ and taking the inverse transform generates the following piece-wise expression for $\psi_{\mathbf{k}}(z)$.

$$\psi_{\mathbf{k}}(z)=\begin{cases}C_1\cosh(qz)+\dfrac{C_2}{q}\sinh(qz), & 0\le z\le z_0\\[2ex] C_1\cosh(qz)+\dfrac{C_2}{q}\sinh(qz)-\dfrac{e^{-ik_x z_0\tan\theta}}{q}\sinh\big(q(z-z_0)\big), & z_0<z\le T\end{cases} \tag{7}$$

The constants $C_1$ and $C_2$ can now be determined from boundary conditions concerning secondary carrier currents directed toward the planes at $z = 0$ and $z = T$. In terms of the inverse relaxation length $\tau$, the secondary carrier currents across any plane of constant $z$ are

$$j_{\text{left}}(z) = \frac{1}{2}\left[\phi\tau + \frac{d\phi}{dz}\right], \qquad j_{\text{right}}(z) = \frac{1}{2}\left[\phi\tau - \frac{d\phi}{dz}\right]. \tag{8}$$

In the right-hand side of the two equations, the first term models the effusion current, while the second term comes from Fick's law. The first boundary condition is determined by the reflectivity $r_0$ of the plane at $z = 0$. Noting that $j_{\text{right}}(0) = r_0 j_{\text{left}}(0)$, one finds

$$\left.\frac{d\phi}{dz}\right|_{z=0} = \tau\rho_0\phi\big|_{z=0}, \qquad \rho_0 \equiv \frac{1-r_0}{1+r_0}. \tag{9}$$

The second boundary condition is determined from the reflectivity $r_1$ of the boundary at $z = T$, as stipulated by the expression $j_{\text{left}}(T) = r_1 j_{\text{right}}(T)$. Defining $\rho_1$ similar to $\rho_0$ and noting that the boundary conditions hold for each Fourier component $\psi_{\mathbf{k}}$ of $\phi$, it can be shown that

$$C_1 = \left[\frac{(q+\tau\rho_1)e^{q(T-z_0)} + (q-\tau\rho_1)e^{-q(T-z_0)}}{(q+\tau\rho_0)(q+\tau\rho_1)e^{qT} - (q-\tau\rho_0)(q-\tau\rho_1)e^{-qT}}\right] e^{-ik_x z_0 \tan\theta}, \tag{10}$$

$$C_2 = \tau\rho_0 C_1. \tag{11}$$

Defining $z = T$ as the plane of the photocathode, the OTF of the scattering process, $T_s(\mathbf{v}, z_0)$, can now be determined for a point source from the expression

$$T_s(\mathbf{v}, z_0) = \left[\frac{\rho_1}{1+\rho_1}\right]\left[\psi_{\mathbf{k}}\tau - \frac{d\psi_{\mathbf{k}}}{dz}\right]_{z=T}, \tag{12}$$

giving

$$T_s(\mathbf{v}, z_0) = \tau\rho_1\left[\frac{(q+\tau\rho_0)e^{(q-ik_x\tan\theta)z_0} + (q-\tau\rho_0)e^{-(q+ik_x\tan\theta)z_0}}{(q+\tau\rho_0)(q+\tau\rho_1)e^{qT} - (q-\tau\rho_0)(q-\tau\rho_1)e^{-qT}}\right]. \tag{13}$$

To calculate the OTF of the entire phosphor, one multiplies Eq. (13) by the relative number of x-ray absorptions as a function of the depth $z_0$

$$N(z_0) = \frac{\mu e^{-\mu z_0 \sec\theta}\sec\theta}{1 - e^{-\mu T\sec\theta}}, \tag{14}$$

where $\mu$ is the x-ray linear attenuation coefficient of the phosphor, and then integrates from $z_0 = 0$ to $z_0 = T$. The OTF is thus

$$T_s(\mathbf{v}) = \frac{\beta\mu\sec\theta}{1 - e^{-\mu T\sec\theta}}\left[\frac{(q+\tau\rho_0)(e^{(\gamma_- - ik_x\tan\theta)T} - 1)}{\gamma_- - ik_x\tan\theta} - \frac{(q-\tau\rho_0)(e^{-(\gamma_+ + ik_x\tan\theta)T} - 1)}{\gamma_+ + ik_x\tan\theta}\right], \tag{15}$$

where

$$\beta \equiv \frac{\tau\rho_1}{(q+\tau\rho_0)(q+\tau\rho_1)e^{qT}-(q-\tau\rho_0)(q-\tau\rho_1)e^{-qT}} \ , \qquad \gamma_{\pm} \equiv q \pm \mu\sec\theta \ . \tag{16}$$

The normalized modulus of the OTF of Eq. (15) gives the modulation transfer function (MTF). In the absence of other noise sources, the quantum NPS or $W_Q(\mathbf{v})$ is calculated by integrating the product of $N(z_0)$ with $|T_s(\mathbf{v}, z_0)|^2$ from $z_0 = 0$ to $z_0 = T$.

$$W_Q(\mathbf{v}) = \frac{\beta^2\mu\sec\theta}{1-e^{-\mu T\sec\theta}}\left[\frac{(q+\tau\rho_0)^2(e^{(q+\gamma_-)T}-1)}{q+\gamma_-}+\frac{2(q^2-\tau^2\rho_0^2)(1-e^{-\mu T\sec\theta})}{\mu\sec\theta}+\frac{(q-\tau\rho_0)^2(1-e^{-(q+\gamma_+)T})}{q+\gamma_+}\right] \tag{17}$$

With Eqs. (15)-(17), one now has all the tools required for determining the DQE of the phosphor. From the work of Nishikawa, DQE can be formulated as the product of four terms [6]

$$\mathrm{DQE}(\mathbf{v}) = A_Q A_S R_C(\mathbf{v}) R_N(\mathbf{v}) \ , \tag{18}$$

where $A_Q$ is the x-ray quantum detection efficiency determined from the Lambert-Beer Law as $1 - e^{-\mu T\sec\theta}$, $A_S$ is the Swank information factor given by $|T_s(\mathbf{0})|^2/W_Q(\mathbf{0})$, $R_C(\mathbf{v})$ is the Lubberts fraction found by normalizing the quotient $|T_s(\mathbf{v})|^2/W_Q(\mathbf{v})$ to unity at $\mathbf{v} = \mathbf{0}$, and $R_N(\mathbf{v})$ is the ratio of the x-ray quantum noise power $W_Q(\mathbf{v})$ to the total noise power $W_T(\mathbf{v})$. Outside of x-ray quantum noise, additional sources of noise which contribute to $W_T(\mathbf{v})$ include optical-detector noise due to silver granules in the phosphor or thermal noise in the photocathode, secondary quantum noise arising from stochastic variation in the number of secondary carriers produced for each incident x-ray, and screen-structure noise [7]. Assuming a quantum-limited imaging system, we treat $R_N(\mathbf{v})$ as unity in this work.

## 3 Results

The preceding results are now illustrated for a phosphor possessing 90% x-ray quantum detection efficiency at normal incidence, a reflective backing, a non-reflective photocathode, and optical scatter at the diffusion limit ($\tau \to \infty$). Assuming that the frequency vector is oriented along the $x$ direction ($v_y = 0$), Figures 1A-1B show MTF and normalized NPS (NNPS) versus frequency at multiple angles of x-ray incidence for a phosphor with no optical absorption ($\sigma = 0$) and a phosphor with high optical absorption ($\sigma = 2T^{-1}$). Figures 1A-1B demonstrate that increasing the optical absorption increases both MTF and NNPS, which is consistent with Swank's prior work at normal incidence. In addition, Figures 1A-1B indicate that increasing the projection angle decreases both MTF and NNPS, with the relative decrease as a function of projection angle being most predominate at high frequencies. The projection angle dependence of the NNPS is slightly less pronounced than the projection angle dependence of the MTF. For example, comparing 30° incidence to normal incidence at 5

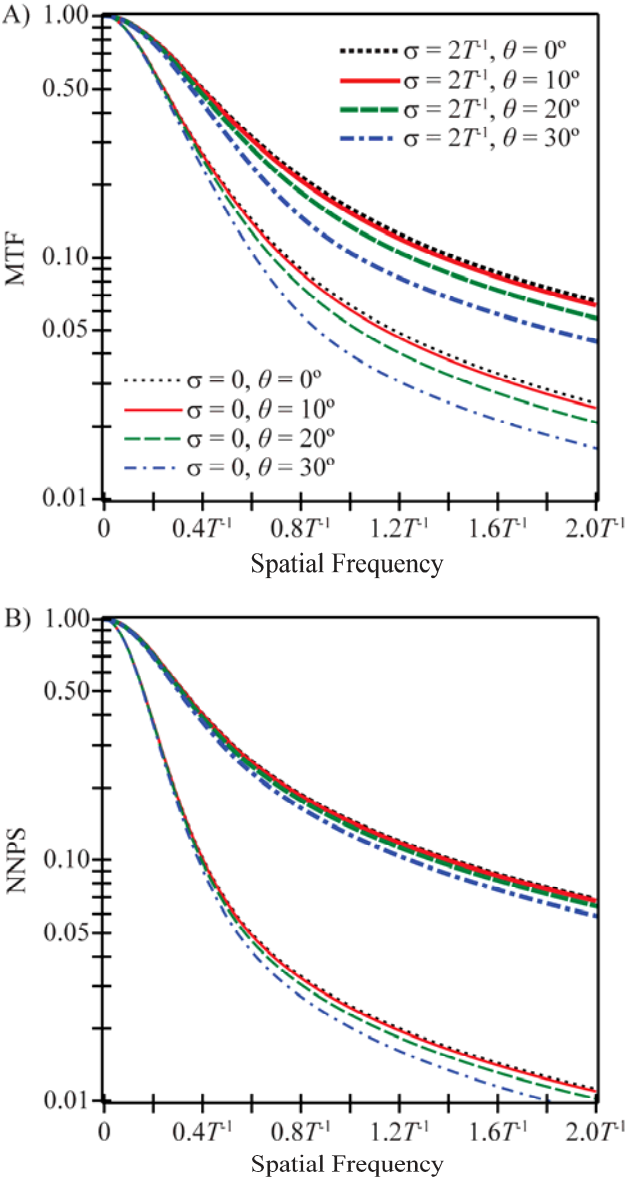


**Fig. 1.** Assuming that the frequency vector is oriented along the $x$ direction, the modulation transfer function (MTF), normalized noise power spectra (NNPS), and detective quantum efficiency (DQE) are plotted versus frequency in units of inverse phosphor thickness ($T^{-1}$) in subplots (A)-(C) for multiple projection angles ($\theta$ = 0°, 10°, 20°, 30°) and two optical absorption parameters ($\sigma$ = 0, $2T^{-1}$). The phosphor possesses 90% x-ray quantum detection efficiency at normal incidence, a reflective backing, a non-reflective photocathode, optical scatter at the diffusion limit, and quantum-limited noise. Subplots (A)-(C) implicitly share a common legend. In (D), the explicit dependence of the Swank information factor ($A_S$) and DQE(**0**) on the angle of x-ray incidence is studied for the two optical absorption parameters.

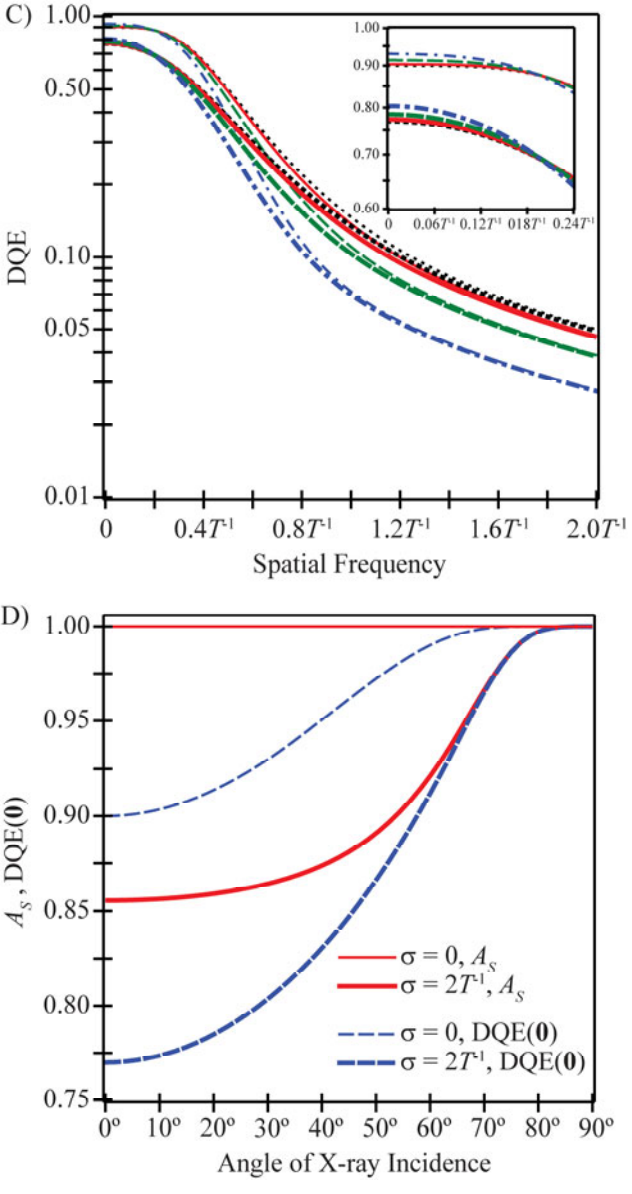


**Fig. 1** (*continued*)

line pairs per millimeter (lp/mm) in a scintillator with 100 μm thickness and no optical absorption, the MTF decreases by 20% whereas the NNPS decreases by only 14% (19% and 8.9%, respectively, with high optical absorption).

Figure 1C shows DQE versus frequency for the same phosphor. Consistent with Swank's previous observations, Figure 1C indicates that increasing the optical absorption reduces the DQE at low frequencies but has a smaller effect on the DQE at high

frequencies. In addition, Figure 1C demonstrates that unlike MTF and NNPS which decrease with projection angle at all frequencies, DQE actually increases with projection angle at low frequencies and only decreases with projection angle at high frequencies. The DQE degradation with projection angle at high frequencies is slightly more pronounced than either the MTF or NNPS degradation. For example, at 5 lp/mm in a scintillator of 100 μm thickness irradiated at a 30° angle, the DQE decreases by 24% relative to normal incidence for both optical absorption parameters shown in the figure.

In Figure 1D, the Swank information factor ($A_S$) and DQE(**0**) are plotted versus the angle of x-ray incidence. Swank has shown that $A_S$ provides a measure of the fluctuation in signal generated from each x-ray due to variability in the absorbed energy of each interacting x-ray and in the number of optical photons generated from each interacting x-ray [8]. Figure 1D demonstrates that in a phosphor with no optical absorption, $A_S$ is unity for all projection angles, but in a phosphor with high optical absorption, $A_S$ increases with projection angle from 0.86 at normal incidence to unity at shearing incidence. In the typical range of projection angles used in DBT, the projection angle dependence of $A_S$ is slight. For example, comparing 30° incidence to normal incidence in a phosphor with high optical absorption, $A_S$ increases by merely 1.0%. Unlike $A_S$, DQE(**0**) is projection angle dependent for all possible optical absorption parameters. The projection angle dependence of DQE(**0**) is more pronounced than the projection angle dependence of $A_S$. In Figure 1D, DQE(**0**) increases from 0.90 (no optical absorption) and 0.77 (high optical absorption) at normal incidence to unity at shearing incidence. Comparing 30° incidence to normal incidence, the relative increase in DQE(**0**) is 3.3% in a phosphor with no optical absorption and 4.4% in a phosphor with high optical absorption.

## 4 Discussion

This work develops analytical models of OTF, NPS, and DQE for a turbid granular phosphor irradiated obliquely. In agreement with Mainprize *et al.* who studied CsI:Tl phosphors experimentally [2], we show that at high frequencies, oblique x-ray incidence gives rise to considerable degradation in MTF and hence poorer resolution. We have also observed that NPS is degraded with projection angle for all frequencies, where the NPS degradation is much less pronounced than the MTF degradation. Although Mainprize *et al.* did not study the dependency of NPS on projection angle, our finding of small changes in NPS with increasing projection angle is qualitatively concordant with the prior work of Hajdok and Cunningham in their Monte Carlo simulations of *a*-Se detectors [3]. As a final point, we have demonstrated that DQE increases with projection angle at low frequencies but decreases with projection angle at high frequencies. Consistent with the observations of Hajdok and Cunningham, the DQE degradation with projection angle at high frequencies is more pronounced than the MTF degradation, reflecting the dependency of DQE on the square of MTF.

In this work, it has been observed that the Swank information factor ($A_S$) is angularly dependent, but its dependency is small over the angles used in DBT. This observation is consistent with Monte Carlo simulations of columnar CsI:Tl phosphors conducted by Badano *et al.*, who show that the variation in $A_S$ over projection angles typical of DBT is minimal [9]. While the relative change in $A_S$ with angle is slim, the

relative increase in DQE(**0**) is more substantial, as it includes the influence of increasing x-ray quantum detection efficiency ($A_Q$) with increasing angle.

**Acknowledgments.** The project described was supported by Grant T32EB009321 from the National Institute of Biomedical Imaging and Bioengineering (NIBIB). The content is solely the responsibility of the authors and does not necessarily represent the official views of the NIBIB or the National Institutes of Health.

## References

1. Rafferty, E.: Tomosynthesis: New Weapon in Breast Cancer Fight. Imaging Economics 17(4) (2004)
2. Mainprize, J.G., Bloomquist, A.K., Kempston, M.P., Yaffe, M.J.: Resolution at oblique incidence angles of a flat panel imager for breast tomosynthesis. Med. Phys. 33(9), 3159–3164 (2006)
3. Hajdok, G., Cunningham, I.A.: Penalty on the detective quantum efficiency from off-axis incident x rays. In: Yaffe, M.J., Flynn, M.J. (eds.) Proc. of SPIE, Medical Imaging 2004: Physics of Medical Imaging, vol. 5368, pp. 109–118. SPIE, Bellingham (2004)
4. Swank, R.K.: Calculation of Modulation Transfer Functions of X-Ray Fluorescent Screens. Appl. Opt. 12(8), 1865–1870 (1973)
5. Marshak, R.E., Brooks, H., Hurwitz Jr., H.: Introduction to the Theory of Diffusion and Slowing Down of Neutrons – I. Nucleonics 4, 10–22 (1949)
6. Nishikawa, R.M., Yaffe, M.J.: Model of the spatial-frequency-dependent detective quantum efficiency of phosphor screens. Med. Phys. 17(5), 894–904 (1990)
7. Nishikawa, R.M., Yaffe, M.J.: Effect of various noise sources on the detective quantum efficiency of phosphor screens. Med. Phys. 17(5), 887–893 (1990)
8. Swank, R.K.: Absorption and noise in x-ray phosphors. J. Appl. Phys. 44(9), 4199–4203 (1973)
9. Badano, A., Kyprianou, I.S., Sempau, J.: Anisotropic imaging performance in indirect x-ray imaging detectors. Med. Phys. 33(8), 2698–2713 (2006)